

## Charge densities and wave functions of chalcogenide deep impurities in Si

Shang Yuan Ren,\* Wei Min Hu,\* Otto F. Sankey, and John D. Dow

*Department of Physics and Materials Research Laboratory, University of Illinois at Urbana-Champaign,  
1110 West Green Street, Urbana, Illinois 61801*

(Received 27 October 1981)

The charge densities of  $S^+$ ,  $Se^+$ , and  $Te^+$  in Si are successfully predicted using an extension of the Hjalmarson *et al.* model of deep impurity levels. The wave functions of these different deep impurity states are all virtually the same.

Analyses of electron nuclear double resonance (ENDOR) and electron-spin-resonance (ESR) spectra of impurities in semiconductors lead directly to the determination of the electronic charge densities of the impurity states.<sup>1</sup> Such data for shallow impurities have been well described by the effective-mass theory of Kohn and Luttinger.<sup>2,3</sup> However, much less is understood about the charge densities of the deep impurity levels that lie more than  $\sim 0.1$  eV from the nearest band edge in the forbidden band gap of a semiconductor. Prototypes of such deep levels are the positively charged S, Se, and Te defects in Si, which produce deep traps near the center of the gap, 590, 520, and 411 meV below the conduction-band edge, respectively.<sup>4</sup> Sixteen years ago Ludwig<sup>3</sup> reported ENDOR spectra for Si:S<sup>+</sup> from which one can extract "experimental" charge densities out to the twelfth neighbor. Recently Grimmeiss *et al.*<sup>4</sup> made similar analyses on ESR data to obtain the central-cell charge densities of Si:Se<sup>+</sup> and Si:Te<sup>+</sup>. The prediction of these deep defect charge densities has proven to be a formidable theoretical task.<sup>5</sup>

The theoretical techniques commonly employed for describing such defects' wave functions are the various self-consistent pseudopotential schemes,<sup>6-9</sup> cluster methods,<sup>5,10</sup> evanescent wave techniques,<sup>11</sup> and the empirical tight-binding scheme of Hjalmarson *et al.*<sup>12</sup> It is widely, but incorrectly, believed that only the laborious, self-consistent methods are capable of producing even qualitatively accurate charge densities. Here we show that the Hjalmarson *et al.* theory, which is the simplest and the most global of the current theories of deep levels, can be extended and modified to yield wave functions and charge densities in excellent quantitative agreement with the "experimental" data of Figs. 1 and 2.<sup>13,14</sup> We find that, to a good approximation, the wave functions of all substitutional

deep impurity levels of the same symmetry are virtually identical—but quite different from shallow-impurity wave functions.

For any substitutional defect with energy  $E$  and in a state  $|\psi\rangle$ , a slight change of the defect potential operator  $V$  produces a change in energy  $dE = \langle \psi | dV | \psi \rangle$ . If, as justified<sup>12,15</sup> by Hjalmarson *et al.*, the defect potential is diagonal in a site representation basis  $|l, \vec{R}, n\rangle$  and localized in the central cell at the origin, i.e.,

$$V = \sum_l |l, \vec{0}, 1\rangle V_l \langle l, \vec{0}, 1| ,$$

then we can relate the amplitude of the deep level's wave function at the impurity site to the infinitesimal changes  $dE$  and  $dV_l$  through

$$\frac{dE}{dV_l} = |\langle l, \vec{0}, 1 | \psi \rangle|^2 . \quad (1)$$

Here  $l$  stands for the irreducible representation of the defect level, either  $A_1$  ( $s$ -like) or  $T_2$  ( $p$ -like), and the integer  $n$  indexes the states transforming according to the  $l$ th irreducible representation at the  $\vec{R}$ th shell. (For  $A_1$  states,  $n$  may be as large as 6 for  $\vec{R}$  within the first 12 shells of neighbors. For example, for  $\vec{R} = \vec{0}$ , there is only the  $n = 1$  basis state, corresponding to the valence  $s$  orbital of the impurity.)

The eigenvalue equation for defect levels in the gap is

$$\det[1 - G(E)V] = 0 , \quad (2)$$

where  $G(E) = (E - H_0)^{-1}$  is the Green's operator and  $H_0$  is the host-crystal Hamiltonian operator. The solution of Eq. (2) for a site-diagonal defect potential reduces to a scalar equation

$$\langle l, \vec{0}, 1 | G | l, \vec{0}, 1 \rangle = 1/V_l . \quad (3)$$

The impurity state  $|\psi\rangle$ , in a localized basis, is

given by

$$\langle l, \vec{R}, n | \psi \rangle = \frac{\langle l, \vec{R}, n | G | l, \vec{0}, 1 \rangle \langle l, \vec{0}, 1 | \psi \rangle}{\langle l, \vec{0}, 1 | G | l, \vec{0}, 1 \rangle} \quad (4)$$

A noteworthy point is that both Eqs. (1) and (4) express the defect wave functions  $\langle l, \vec{R}, n | \psi \rangle$  as functions of the impurity energy  $E$  alone, and do not depend explicitly on the defect potential  $V$ . Hence the difficult problem of accurately determining the defect potential (including, to an extent,<sup>15</sup> its dependence on lattice relaxation around the defect, and the charge state of the defect) is circumvented.

We represent the host Hamiltonian by the nearest-neighbor  $sp^3s^*$  ten-state model of Vogl *et al.*<sup>16</sup> In order to make contact with the ENDOR and ESR experiments, we take

$$|\langle l, \vec{R}, n | \psi \rangle|^2 = |\psi_{l,n}(\vec{R})|^2 / B,$$

where we have  $B = |\psi_{l}(\text{free atom})(\vec{0})|^2$  for  $\vec{R} = \vec{0}$ ; for  $\vec{R} \neq \vec{0}$ ,  $B$  is a known function of the Si free atom values of  $|\psi(\vec{0})|^2$  and  $\langle r^{-3} \rangle$  (Ref. 13 discusses how  $B$  is determined).

The basis states  $|l, \vec{R}, n\rangle$  are (formally) symmetrically orthogonalized, symmetrized Löwdin orbitals. (We do not actually need to evaluate the basis orbitals  $\langle \vec{r} | l, \vec{R}, n \rangle$  in the present work.) For example,  $|A_1, \vec{0}, 1\rangle$  means the  $A_1$  symmetric linear combination of the four  $sp^3$  hybrids at the impurity site<sup>17</sup>;  $|A_1, \vec{R}_1, 1\rangle$  is the  $A_1$  combination of four inward-directed Löwdin hybrids centered at the nearest-neighbor sites,<sup>18</sup> and  $|A_1, \vec{R}_1, 2\rangle$  is constructed from the twelve outward-directed hybrids at the nearest-neighbor sites,<sup>19</sup> and so on.

The isotropic part<sup>14</sup> of the  $S^+$  deep-level wave function (Fig. 1) was calculated for a defect with an energy 590 meV below the conduction-band edge, as observed for  $S^+$  in Si.<sup>20</sup> The agreement between theory and data is gratifying. Even the small discrepancy between theory and data for  $R > 6.5 \text{ \AA}$  can be readily understood: The Coulomb interaction omitted from the model causes the impurity's wave function to have an effective-mass tail (which has the observed  $R$  dependence; see Fig. 1) for these large values of  $R$ . For  $R < 6.5 \text{ \AA}$ , the deep-level wave function is strikingly different from the effective-mass approximation wave function.

We have also calculated the anisotropic part<sup>13</sup> of the  $S^+$  deep-level wave function; for example, at the first neighbor we find an amplitude of  $-0.67$  versus the measured value of  $\pm 0.69$  and an effective-mass theory value of zero.

The wave functions and charge densities com-

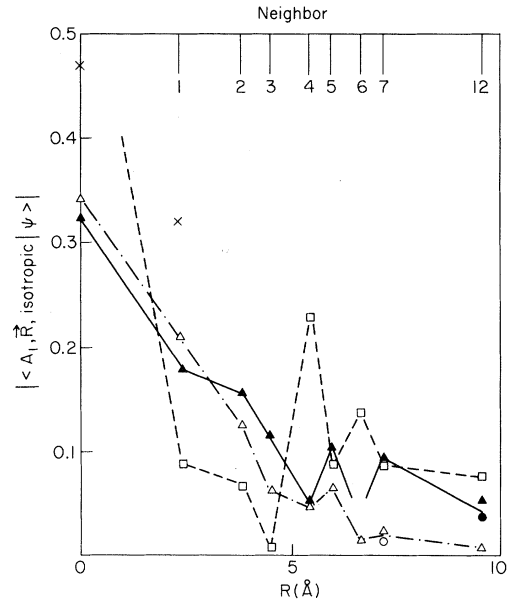


FIG. 1. Magnitude of the isotropic part (Ref. 14) of the wave function of a  $S^+$  impurity in Si,  $|\langle A_1, \vec{R}, \text{isotropic} | \psi \rangle|$ , as a function of the distance  $R$  (in angstroms) from the origin (impurity site). The solid triangles and solid circles are derived from ENDOR data of Ref. 3, using atomic parameters of  $^{29}\text{Si}$  and  $^{33}\text{S}$  determined in Ref. 13. The open triangles and open circles are our calculated results. Some shells of atoms have two distinct subshells which transform into themselves only under the operations of the tetrahedral group, giving rise to both triangles and circles. The crosses are calculated results of Ref. 5. The dashed line and open squares represent the effective-mass approximation (Ref. 3). The positions of the neighbors are indicated at the top of the figure.  $\langle A_1, \vec{R}, \text{isotropic} | \psi \rangle$  is predicted to be negative at the first, second, fifth, seventh, and twelfth neighbors. Neither data nor predictions are given for the eighth through the eleventh neighbors. The solid (chained) line merely connects the solid (open) triangles.

puted here lend quantitative support to the idea of the hostile nature of many deep level wave functions (an idea that is implied by the notion of hyperdeep levels<sup>12</sup>). Figure 2 shows  $\langle A_1, \vec{0}, 1 | \psi \rangle$ ,  $\langle A_1, \vec{R}_1, 1 | \psi \rangle$ , and  $\langle A_1, \vec{R}_1, 2 | \psi \rangle$  as functions of the deep-level energy  $E$  for defects in Si. The on-site wave functions  $\langle A_1, \vec{0}, 1 | \psi \rangle$  are not very different for all deep defects, ranging from 0.27 to 0.36, indicating that they depend very little on the defect. And the first-neighbor amplitudes  $\langle A_1, \vec{R}_1, 1 | \psi \rangle$  are negative and approximately twice as large in magnitude as the central-site amplitudes, and likewise insensitive to the impurity (lying between  $-0.73$  and  $-0.54$ ), again showing

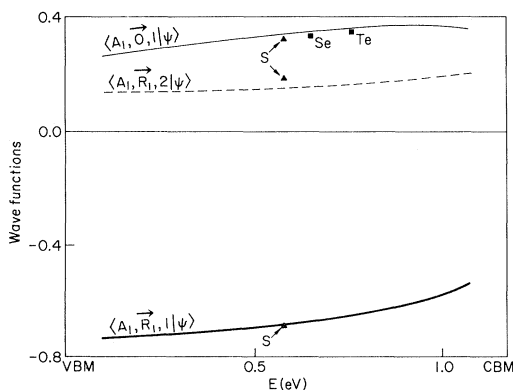


FIG. 2. On-site wave function  $\langle A_{1, \vec{0}, 1} | \psi \rangle$  (thin solid line) and first shell wave functions  $\langle A_{1, \vec{R}_1, 1} | \psi \rangle$  (thick solid line) and  $\langle A_{1, \vec{R}_1, 2} | \psi \rangle$  (dashed line) are shown as functions of the deep impurity energies  $E$  (in eV). Data for  $S^+$  are from Ref. 3 (solid triangles); data for  $Se^+$  and  $Te^+$  (solid squares) are from Ref. 4, with the values of  $|\psi(\vec{0})|^2$  and  $\langle r^{-3} \rangle$  determined or corrected according to Ref. 13. We have chosen the sign of  $\langle A_{1, \vec{0}, 1} | \psi \rangle$  to be positive, which determines the sign of  $\langle A_{1, \vec{R}, n} | \psi \rangle$  for all  $\vec{R}$ . VBM and CBM on the abscissa refer to the valence-band maximum ( $E=0.0$ ) and the conduction-band minimum ( $E=1.17$  eV in this model).

that the deep level is antibonding and hostlike—and not impuritylike. In the sense of Ref. 12, these levels are “pinned” to the ideal vacancy level.

Previous efforts to calculate these spectra using a sophisticated linear combination of atomic orbitals theory for a cluster of 275 atoms have been less successful in describing the data.<sup>5</sup> We do not

know the origin of this discrepancy, but speculate that it might be reduced by including more orbitals in the basis set.

One reason why moderate-sized cluster calculations in general give less reliable charge densities is that much of the defect wave function lies outside all but the largest clusters. For example, by our calculation, more than 30% of the charge density of every substitutional  $A_1$  deep level in Si lies outside a cluster of 87 atoms (seventh-neighbor shell).<sup>21</sup>

In summary, we have shown (i) that the ENDOR and ESR data for  $S^+$ ,  $Se^+$ , and  $Te^+$  in Si can be accounted for quantitatively with a very simple theory, (ii) that the wave functions of all three of these  $sp^3$ -bonded deep levels are virtually the same, but quite different from shallow-level wave functions, and (iii) that the wave functions can be evaluated simply, knowing only the (observed) deep-level energy  $E$ , and without any explicit knowledge of the defect potential. Thus, we predict that two  $sp^3$ -bonded deep levels of the same symmetry and of approximately the same energy, but associated with different impurities and different charge states, can be expected to have similar wave functions.

We gratefully acknowledge the financial support of the Office of Naval Research (Contract No. N00014-77-C-0537) and helpful discussions with H. P. Hjalmarsen, P. Vogl, D. J. Wolford, G. Baraff, M. Stoneham, and Y. C. Chang. We thank the authors of Ref. 4 for sending us a copy of their manuscript prior to publication.

\*Permanent address: Department of Physics, University of Science and Technology of China, Hefei, China.

<sup>1</sup>G. Feher, Phys. Rev. **114**, 1219 (1959).

<sup>2</sup>W. Kohn and J. M. Luttinger, Phys. Rev. **97**, 1721 (1955); **98**, 915 (1955).

<sup>3</sup>G. W. Ludwig, Phys. Rev. A **137**, 1520 (1965).

<sup>4</sup>H. G. Grimmeiss, E. Janzén, H. Ennen, O. Schirmer, J. Schneider, R. Wörner, C. Holm, E. Sirtl, and P. Wagner, Phys. Rev. B **24**, 4571 (1981).

<sup>5</sup>T. Shimizu and K. Minami, Phys. Status Solidi B **48**, K181 (1971).

<sup>6</sup>M. Jaros and S. Brand, Phys. Rev. B **14**, 4494 (1976); M. Jaros, C. O. Rodriguez, and S. Brand, *ibid.* **19**, 3137 (1979).

<sup>7</sup>G. A. Baraff and M. Schlüter, Phys. Rev. Lett. **41**, 892 (1978); Phys. Rev. B **19**, 4965 (1979).

<sup>8</sup>J. Bernholc, N. O. Lipari, and S. T. Pantelides, Phys. Rev. Lett. **41**, 895 (1978); Phys. Rev. B **21**, 3545 (1980).

<sup>9</sup>M. Scheffler and S. T. Pantelides (private communication) have recently studied the magnetic susceptibilities of deep levels. Their work has some elements in common with the present work.

<sup>10</sup>L. A. Hemstreet, Phys. Rev. B **15**, 834 (1977); **22**, 4590 (1980).

<sup>11</sup>K. J. Blow and J. C. Inkson, J. Phys. C **13**, 359 (1980).

<sup>12</sup>H. P. Hjalmarsen, P. Vogl, D. J. Wolford, and J. D. Dow, Phys. Rev. Lett. **44**, 810 (1980). See also W. Y. Hsu, J. D. Dow, D. J. Wolford, and B. G. Streetman, Phys. Rev. B **16**, 1597 (1977).

<sup>13</sup>See Eqs. (9)–(12) and Appendix A of G. D. Watkins and J. W. Corbett, Phys. Rev. **134**, A1359 (1964).

<sup>14</sup>The isotropic part is given by

$$|A_{1, \vec{R}, \text{isotropic}}\rangle = \sum_{n=1}^3 |A_{1, \vec{R}, n}\rangle f_n,$$

where we have the following values for the vector  $\vec{f}$ , for  $\vec{R}$  being the zeroth through the fifth neighbor:

(1,0,0), (1/2,√3/2,0), (1/2,1/2,√2/2), (1/2,1/2,√2/2), (√2/2,√2/2,0), and (1/2,1/2,√2/2). Results are not reported for the eighth through the eleventh neighbors. For the sixth, seventh, and twelfth neighbors, there are two isotropic parts of  $|\psi\rangle$  with coefficients (1/2,1/2,√2/2) and (1/2,1/2,√2/2), (1/2,1/2,√2/2) and (1/2,√3/2,0), and (1/2,√3/2,0) and (1/2,√3/2,0), respectively.

<sup>15</sup>The corrections to defect levels due to the non-central-cell defect potential have been estimated to be only a few tenths of an eV in Ref. 12 and by using the paired-defect theory of O. F. Sankey, H. P. Hjalmarson, J. D. Dow, D. J. Wolford, and B. G. Streetman, Phys. Rev. Lett. **45**, 1656 (1980).

<sup>16</sup>P. Vogl, H. P. Hjalmarson, and J. D. Dow, J. Phys. Chem. Solids (in press).

<sup>17</sup>These states can be expressed in terms of the (outward) directed-valence hybrids  $|h_i^{\vec{0}}\rangle$  centered at the origin:

$$|A_1, \vec{0}, 1\rangle = (|h_1^{\vec{0}}\rangle + |h_2^{\vec{0}}\rangle + |h_3^{\vec{0}}\rangle + |h_4^{\vec{0}}\rangle)/2,$$

where  $i = 1, 2, 3,$  and  $4$  labels the hybrid vectors  $\vec{c} = (1, 1, 1)/2, (1, -1, 1)/2, (1, -1, -1)/2,$  or  $(1, 1, -1)/2$ . The hybrids are expressed in terms of the basis orbitals centered at  $\vec{R}$  as

$$|h_i^{\vec{R}}\rangle = c_1 |s\rangle + c_2 |p_x\rangle + c_3 |p_y\rangle + c_4 |p_z\rangle.$$

<sup>18</sup>We have

$$|A_1, \vec{R}_1, 1\rangle = (|h_1^{\vec{a}}\rangle + |h_2^{\vec{b}}\rangle + |h_3^{\vec{c}}\rangle + |h_4^{\vec{d}}\rangle)/2,$$

where  $\vec{a}, \vec{b}, \vec{c},$  and  $\vec{d}$  refer to the nearest-neighbor sites  $(a_L/4)(1, 1, 1), (a_L/4)(-1, 1, -1), (a_L/4)(-1, -1, 1),$  and  $(a_L/4)(1, -1, -1)$ ; 1, 2, 3, and 4 denote hybrids centered at the neighboring sites with  $\vec{c} = (1, -1, -1)/2, (1, 1, -1)/2, (1, 1, 1)/2,$  and  $(1, -1, 1)/2$ .

<sup>19</sup>We have

$$\begin{aligned} |A_1, \vec{R}_1, 2\rangle = & (|h_2^{\vec{a}}\rangle + |h_3^{\vec{a}}\rangle + |h_4^{\vec{a}}\rangle + |h_1^{\vec{b}}\rangle \\ & + |h_3^{\vec{b}}\rangle + |h_4^{\vec{b}}\rangle + |h_1^{\vec{c}}\rangle + |h_2^{\vec{c}}\rangle \\ & + |h_4^{\vec{c}}\rangle + |h_1^{\vec{d}}\rangle + |h_2^{\vec{d}}\rangle \\ & + |h_3^{\vec{d}}\rangle)/\sqrt{12}, \end{aligned}$$

where  $\vec{a}, \vec{b}, \vec{c},$  and  $\vec{d}$  and 1, 2, 3, and 4 have the same meanings as in Ref. 18.

<sup>20</sup>H. G. Grimmeiss, E. Janzén, and B. Skarstam, J. Appl. Phys. **51**, 4212 (1980).

<sup>21</sup>Here we use the conventional definition that a level is deep if it lies in the gap more than 0.1 eV from the nearest band edge. Some levels closer to the band edge are actually "deep" in the localization sense of Ref. 12.